JOURNAL OF VIROLOGY, Mar. 2011, p. 2112–2125 Vol. 85, No. 5
0022-538X/11/$12.00 doi:10.1128/JVI.01931-10

Comparative Analysis of Monkeypox Virus Infection of Cynomolgus Macaques by the Intravenous or Intrabronchial Inoculation Route▽

Reed F. Johnson,[1]†* Julie Dyall,[2]† Dan R. Ragland,[2] Louis Huzella,[2] Russell Byrum,[2] Catherine Jett,[2] Marisa St. Claire,[2] Alvin L. Smith,[1] Jason Paragas,[2] Joseph E. Blaney,[1] and Peter B. Jahrling[1,2]

Emerging Viral Pathogens Section, National Institute of Allergy and Infectious Diseases, National Institutes of Health, Bethesda, Maryland 20892,[1] and Integrated Research Facility, National Institute of Allergy and Infectious Diseases, National Institutes of Health, Frederick, Maryland 21702[2]

Received 11 September 2010/Accepted 17 November 2010

Monkeypox virus (MPXV) infection has recently expanded in geographic distribution and can be fatal in up to 10% of cases. The intravenous (i.v.) inoculation of nonhuman primates (NHPs) results in an accelerated fulminant disease course compared to that of naturally occurring MPXV infection in humans. Alternative routes of inoculation are being investigated to define an NHP model of infection that more closely resembles natural disease progression. Our goal was to determine if the intrabronchial (i.b.) exposure of NHPs to MPXV results in a systemic disease that better resembles the progression of human MPXV infection. Here, we compared the disease course following an i.v. or i.b. inoculation of NHPs with 10-fold serial doses of MPXV Zaire. Classical pox-like disease was observed in NHPs administered a high virus dose by either route. Several key events were delayed in the highest doses tested of the i.b. model compared to the timing of the i.v. model, including the onset of fever, lesion appearance, peak viremia, viral shedding in nasal and oral swabs, peak cytokine levels, and time to reach endpoint criteria. Virus distribution across 19 tissues was largely unaffected by the inoculation route at the highest doses tested. The NHPs inoculated by the i.b. route developed a viral pneumonia that likely exacerbated disease progression. Based on the observations of the delayed onset of clinical and virological parameters and endpoint criteria that may more closely resemble those of human MPXV infection, the i.b. MPXV model should be considered for the further investigation of viral pathogenesis and countermeasures.

Monkeypox virus (MPXV) is a member of the genus *Orthopoxvirus*, which includes variola (VARV), cowpox, vaccinia, and camelpox viruses. MPXV was first isolated in 1958 in Denmark from an imported cynomolgus macaque, and the initial reported human cases were described in the early 1970s in central Africa (1, 2). Prior to smallpox eradication, human MPXV infections likely were misdiagnosed as variola virus infections due to the prevalence of variola virus and the similarity of disease presentation (22). While variola virus, the causative agent of smallpox, was restricted to human-to-human transmission, MPXV is a zoonotic disease of primarily central Africa that is maintained in a rather broad animal reservoir, including squirrels and other rodents (7, 18). In humans, incidental MPXV infection is characterized by marked lymphadenopathy and shares many features of variola disease, including high fever, headache, malaise, and lesion development. While MPXV disease in humans is considered to be less severe than disease associated with smallpox, case fatality rates of up to 10% have been reported with outbreaks caused by viruses of the virulent central African clade (25). In contrast, western African clades are associated with less severe infection in humans and nonhuman primates (NHPs) (6, 34). The majority of human MPXV infections are attributed to close contact with animal carriers of the virus, and MPXV transmission between humans is considerably less efficient than variola virus transmission (35, 41). Secondary attack rates of MPXV in nonvaccinated household members were reported to be 9%, whereas that for variola virus was 58% (28). However, a recent report detailed an outbreak where six degrees of transmission from a single case were reported in a hospital, highlighting the public health threat of MPXV (24).

Several factors have led to a recent increase in research efforts to understand the pathogenesis of MPXV and other orthopoxviruses and to identify countermeasures to these agents. First, MPXV is a classical case of an emerging zoonotic disease, as the reported incidence and geographical range of disease in Africa has increased during the past three decades (28). In 2009, the World Health Organization reported 1,379 MPXV cases, with 21 fatalities (1.5% case fatality rate) (42). Recently, Rimoin et al. have demonstrated that the incidence of MPXV has increased since the cessation of VARV vaccination, and the increase is observed in the unvaccinated population in the area in which it is endemic, supporting the importance of MPXV as an emerging infectious disease and the necessity for improved countermeasures (32). Further support for the emergence of MPXV occurred during a 2003 outbreak of roughly 70 MPXV cases in the United States that was traced to contact with domestic prairie dogs that were exposed to MPXV-infected imported rodents (29). Overall, the severity of disease in the United States was relatively mild, although 26 patients were hospitalized, and likely could be attributed to the lower virulence of the western African strain that caused the outbreak. A second factor that has accelerated

* Corresponding author. Mailing address: National Institutes of Health, NIAID/EVPS, Bldg 33, Rm 2E19A, 33 North Dr., Bethesda, MD 20892. Phone: (301) 443-5700. Fax: (301) 480-3322. E-mail: johnsonreed@mail.nih.gov.
† These authors contributed equally.
▽ Published ahead of print on 8 December 2010.

MPXV research is the concern that MPXV or variola virus could be used as an agent of bioterrorism (20, 28). The intentional release of variola virus or even a virulent MPXV strain into an increasingly nonvaccinated population would result in a severe public health emergency, and currently insufficient countermeasures exist. Finally, while variola virus research is highly restricted, MPXV serves as an excellent surrogate virus for study, since disease caused by the viruses is similar in presentation.

Several recent studies have used NHP models of MPXV infection to evaluate anti-orthopoxvirus vaccines and antivirals and to investigate viral pathogenesis (8, 10, 11, 16, 36, 38, 39, 40, 43). The majority of these studies have used the intravenous (i.v.) inoculation of 5×10^7 PFU of central African strains of MPXV. While the i.v. infection of NHPs causes severe lesional disease, results in considerable morbidity, and has proven to be a useful model, it does not optimally reflect authentic human disease. The i.v. administration of this high viral dose appears to eclipse the incubation period of approximately 10 to 12 days that is observed in humans, resulting in an accelerated fulminant disease. Furthermore, the natural route of variola virus transmission and secondary MPXV transmission in humans is primarily by respiratory exposure (1). Therefore, investigations using aerosol (43), intratracheal (i.t.) (39, 40), and intranasal (i.n.) (34) MPXV administration recently have been reported, which may comprise elements that improve upon the i.v. model. The importance of identifying an optimal animal model to characterize MPXV pathogenesis and test countermeasures has been reinforced by two draft guidance documents from the Food and Drug Administration pertaining to the "Animal Rule" that indicate that the route and dosage of administration, quantification of exposure, time to onset of disease, and time course/progression of disease are critical factors for the determination of the suitability and acceptability of an animal model for efficacy studies (http://www.accessdata.fda.gov/scripts/cdrh/cfdocs/cfcfr/CFRSearch.cfm?CFRPart=314&showFR=1&subpartNode=21:5.0.1.1.4.9).

In the current study of MPXV disease in cynomolgus macaques, we sought to (i) expand our understanding of the clinical, virological, immunological, and histopathological parameters and dose response of i.v. infection, (ii) determine the potential utility of intrabronchial (i.b.) infection as an improved model of simulated respiratory infection with a potentially slower progression of disease, and (iii) compare the disease sequelae of this novel respiratory exposure to that of i.v. exposure. The i.b. inoculation of NHPs has been reported to be an effective method for the delivery of simian varicella virus, adenovirus vectors, and *Mycobacterium tuberculosis* (4, 23, 27). Inoculation by the i.b. route appears to be a consistent and repeatable method of inocula delivery, because administration is based on anatomical landmarks and the quantity of inocula can be readily measured and completely administered. In addition, the equipment required for the procedure, a pediatric bronchoscope, is relatively inexpensive compared to aerosolization equipment, and veterinary staff commonly are experienced in the procedure. Here, we compare the clinical disease and pathogenesis of i.v. and i.b. infection and relate the results to existing models of orthopoxvirus infection and human disease.

MATERIALS AND METHODS

Virus and cells. MPXV Zaire 79 strain was propagated in Vero E6 cells at a multiplicity of infection (MOI) of 0.1 for 7 days. Vero E6 cells were maintained in Dulbecco's modified essential medium (DMEM) (HyClone, Logan, UT) supplemented with 10% fetal bovine serum (FBS) (HyClone, Logan, UT) and 1% penicillin and streptomycin at 37°C with 5% CO_2. BSC-1 cells were maintained in MEM supplemented with 10% FBS and 1% penicillin and streptomycin at 37°C with 5% CO_2. Inoculum for challenge experiments was prepared by the disruption of Vero E6 cells in an ultrasonic processor VCX-750 (Sonics and Materials, Newtown, CT) for 120 s at 40% power on ice, followed by centrifugation ($500 \times g$ for 10 min at 4°C).

Challenge of NHPs. Cynomolgus macaques (*Macaca fascicularis*) of both sexes, ranging in size from 3 to 6 kg, were housed in biosafety level 3 containment. Prior to enrollment, NHPs were screened for simian retrovirus (SRV), simian T-lymphotrophic virus (STLV), MPXV, vaccinia virus (VACV), and cowpox virus by quantitative PCR. In addition, NHPs had no detectable neutralizing antibody activity against VACV, as determined by the flow-cytometric assay described below (9). All animal procedures were approved by the National Institute of Allergy and Infectious Diseases Animal Care and Use Committee and adhered to National Institutes of Health (NIH) policies.

For i.v. inoculation, NHPs were anesthetized with telazol, and 1 ml of virus inoculum was injected into the saphenous vein with a 21-gauge needle. Serial 10-fold dilutions of MPXV from 5×10^7 to 5×10^4 PFU were administered to groups of six (5×10^7 and 5×10^6 PFU) or three (5×10^5 and 5×10^4 PFU) NHPs. For i.b. inoculation, NHPs were anesthetized as described above, and inocula were delivered by placing a pediatric bronchoscope into the left tertiary bronchus. One ml of inoculum was placed into the bronchoscope's sampling port and flushed with 2 ml sterile phosphate-buffered saline (PBS) and 5 ml of air. Serial 10-fold dilutions of MPXV from 5×10^6 to 5×10^4 PFU were administered to groups of six (5×10^5 PFU) or three NHPs (5×10^6 and 5×10^4 PFU).

Challenged NHPs were monitored twice daily for clinical signs of disease. Physical exams (PE), including the monitoring of temperature, weight, and lesion count, were performed on study day −7, 0, 3, 5, 7, 9, 11, 14, 16, 20, 22, and 36 or study day −7, 0, 2, 4, 6, 8, 10, 12, 16, 21, and 36. On PE days, oral and nasal swabs and blood were collected and assayed for viral load. Blood samples also were assayed for complete blood count analysis, serum chemistry levels, and cytokine levels. Peripheral blood mononuclear cells (PBMCs) were isolated for flow-cytometric analysis as described below. Lesional disease was monitored by the enumeration of skin lesions and the classification of lesions into stages from macular to scab for each NHP at physical exam. Coalescing lesions were counted as one when discrete borders could no longer be observed.

Hematology and blood biochemistry. PBMCs were isolated from whole blood as follows. EDTA-collected blood tubes were centrifuged at 2,400 rpm for 10 min. The buffy coat was removed, diluted 3× in PBS, and layered over 100% Histopaque. PBMCs were centrifuged at 1,400 rpm for 30 min without braking, removed, and washed with PBS plus 2% FBS. PBMCs then were pelleted and stored in FBS plus 10% dimethylsulfoxide (DMSO) at −80°C. For flow-cytometric analysis, PBMCs were thawed at room temperature, washed with PBS plus 2% FBS, and pelleted at 1,500 rpm for 10 min. Samples were surface stained with a custom antibody cocktail (BD Biosciences, Franklin Lakes, NJ) for CD3, CD4, CD8, CD14, CD16, CD20, and CD45 for 30 min, washed with PBS plus 2% FBS, and pelleted at 8,000 rpm for 2 min. Cells then were fixed with 0.1% paraformaldehyde, and data were collected on an LSRII (BD Biosciences Franklin Lakes NJ) and analyzed by FlowJo v8.6.3 (TreeStar Inc., Ashland, OR). Monocytes were identified by gating on CD45 and CD14. T cells were gated on CD45, then on CD3, and then on either $CD4^+$ or $CD8^+$ for analysis.

Quantification of viremia by qPCR. Viral load in whole blood was determined by quantitative PCR (qPCR) after DNA isolation using Genfind v2 according to the manufacturer's directions (Agencourt, Danvers, MA). Isolated DNA was screened for the presence of the MPXV HA gene with a LightCycler apparatus (Roche, Basel, Switzerland). Five μl of isolated DNA was incubated with 15 μl of reaction mix (10 μl of MasterMix, 4.5 μl of ultrapure water, and 0.5 μl primers directed at the HA [B2R] gene) (37). Thermal cycling for the LightCycler was performed as follows: 1 cycle at 95°C for 5 min, followed by 45 cycles of 95°C for 10 s and 60°C for 20 s. A fluorescence reading was taken at the end of each 60°C step. Each reaction capillary tube was read in channel 1 (F1) at a gain setting of 16, with data analysis performed using the LightCycler data analysis software (version 3.5.3). Sample curves were analyzed by using the second derivative maximum with the baseline adjustment set to arithmetic. The limit of detection was 10 gene copies per ml.

Plaque assay. The level of infectious virus in tissue samples was assayed by plaque assay on BSC-1 cell monolayers. Briefly, 10-fold serial dilutions of 10%

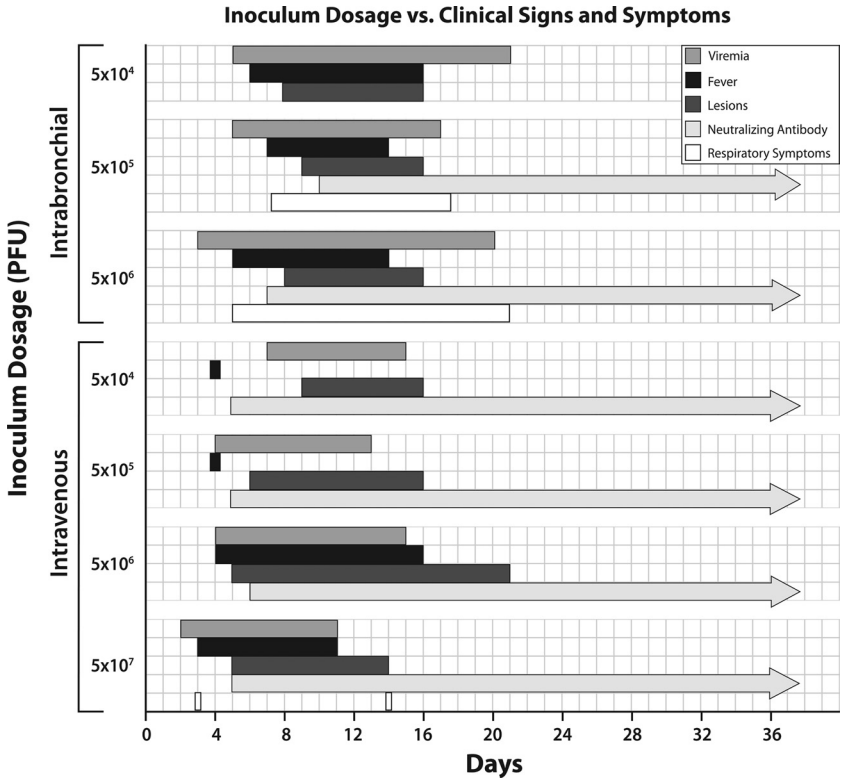

FIG. 1. Course of disease progression in NHPs inoculated with MPXV. The duration of fever, lesions, viremia, neutralizing antibody activity, and respiratory symptoms were compared among groups receiving various doses of MPXV by the i.v. and i.b. routes. Respiratory symptoms include increased respiratory rate, decreased SpO_2%, or dyspnea. Bars represent the mean day of the onset of the criteria to the mean day of the resolution of the criteria.

tissue homogenates were incubated with BSC-1 cells in 12-well plates. After 1 h of adsorption, cells were overlaid with 1.6% agarose and 2× MEM (mixed 1:1) and incubated at 37°C for 3 to 4 days. Following incubation, agarose plugs were removed, the monolayers were stained with crystal violet (0.1% crystal violet, 20% ethanol, vol/vol), and plaques were enumerated. More than 60 tissues from each moribund NHP were evaluated, and the tissues with the highest and most consistent levels of virus replication are described here.

Neutralizing antibody assay. The level of neutralizing antibodies in MPXV-infected NHPs was measured by a flow-cytometric assay using a VACV expressing green fluorescent protein (VACV-GFP) as the target virus (9). In triplicate, serum samples (diluted 1:1,000) from each physical exam day and target virus (MOI of 2.5) were allowed to complex for 1 h at 37°C. The serum and virus mixtures were added to 5×10^4 CV-1 cells and treated with 44 μg/ml of cytosine arabinoside. Infected cells were incubated for 24 h, followed by trypsinization (trypsin plus 2.5% EDTA), washed twice in PBS plus 2% FBS, and analyzed by flow cytometry for GFP expression using a Fortessa (BD Biosciences, Franklin Lakes, NJ) and analyzed with FlowJo 8.6.3 (TreeStar Inc., Ashland, OR). The percentage of the inhibition of fluorescence is a relative indicator of the neutralizing antibody activity in a given serum sample.

Cytokine and chemokine quantification. The level of 23 cytokines and chemokines in NHP sera was analyzed using the Millipore nonhuman primate cytokine panel premixed 23-plex (Millipore, Billerica, MA). Briefly, plasma samples were transferred to a 96-well plate and incubated with beads coated with antibodies directed against different cytokines or chemokines. For RANTES, a 1:100 dilution was made for each sample. Following incubation, the beads were washed, incubated with anti-cytokine and -chemokine antibodies, and incubated with streptavidin-R-phycoerythrin (SAV/RPE). Beads were assayed on the Luminex 100/200 System (Bio-Rad, Hercules, CA). Cytokines were included for comparison when there was a 2-fold or greater measurable response within a group of NHPs.

Necropsy. Complete necropsies were performed after moribund animals, which met clinical endpoint criteria, were humanely euthanized. Animals that survived infection were euthanized and necropsied at 36 days postexposure. Tissue samples were collected as required for histopathological analysis and the determination of viral load.

Histology and immunohistochemistry. Tissues were immersion fixed in 10% phosphate-buffered formalin for a minimum of 14 days. Samples then were paraffin embedded and sectioned to 4 μm by a microtome. Fixed slides then were stained with hematoxylin and eosin (H&E) and examined by light microscopy. Immunohistochemistry (IHC) assays were performed on a Bond Immunostainer. Briefly, approximately 4-μm sections of tissue on glass slides were deparaffinized and rehydrated, and antigen retrieval was performed on the Bond Immunostainer. Sections then were treated with the Bond polymer refine detection system. Positive controls included formalin-fixed, paraffin-embedded spleen, lymphoid tissue, or skin from NHPs infected with monkeypox virus and known to contain high reactivity. Negative controls included spleen or lymphoid tissue from uninfected NHPs.

RESULTS

Clinical presentation of disease. Groups of three to six cynomolgus macaques were infected with serial 10-fold dilutions of MPXV Zaire 79 by the i.v. route (5×10^7 to 5×10^4 PFU) or by the i.b. route (5×10^6 to 5×10^4 PFU). While 5×10^7 PFU is the standard dose in the established lethal MPXV i.v. model and consequently of particular interest here, this dosage was not attempted by i.b. inoculation, because we have previously demonstrated that NHPs infected i.b. with 5×10^7 PFU cowpox virus develop fulminant pneumonia without a typical poxviral disease course (A. L. Smith et al., unpublished data). An overview of the disease progression and clinical signs are provided in Fig. 1. Severe disease that resulted in NHPs meeting

TABLE 1. Comparison of intravenous and intrabronchial MPXV inoculation

Dose (PFU)	i.v. inoculation				i.b. inoculation			
	No. moribund[a]/no. challenged	Mean day of end point[b] (range)	Mean peak viremia[c] (log_{10} gene copies/ml) (range)	Mean day of peak viremia (range)	No. moribund/no. challenged	Mean day of endpoint (range)	Mean peak viremia (log_{10} gene copies/ml) (range)	Mean day of peak viremia (range)
5×10^7	5/6	9.8 (7–13)	8.3 (6.5–8.9)	8.2 (5–11)	Not done			
5×10^6	1/6	15.0 (NA)	6.4 (NA)	9.3 (NA)	2/3	20.0 (19–21)	7.2 (6.7–7.6)	13.7 (9–16)
5×10^5	0/3	NA	5.4 (4.6–5.7)	6 (4–8)	1/6	9.0 (NA)	8.5 (5.4–9.3)	9.5 (7–11)
5×10^4	0/3	NA	4.9 (4.1–5.3)	9.3 (8–12)	0/3	NA	5.9 (5.2–6.2)	10.0 (8–12)

[a] Moribund was defined as reaching end point criteria, resulting in euthanasia.
[b] Mean day of death was calculated by averaging the days on which animals within a group became moribund. NA, not applicable.
[c] Viremia was determined by quantitative PCR analysis of DNA isolated from whole blood, and mean peak viremia was calculated by averaging the peak viremia for each animal within a group.

endpoint criteria was observed in 83 and 15% of NHPs challenged i.v. with 5×10^7 and 5×10^6 PFU, respectively (Table 1). In NHPs challenged by the i.b. route, 66% of NHPs in the 5×10^6-PFU group and 15% of NHPs in the 5×10^5-PFU group succumbed to disease. Importantly, the time to endpoint criteria was two times longer for the NHPs infected with 5×10^6 PFU i.b. (20.0 days) compared to those for NHPs infected with the standard lethal i.v. dose of 5×10^7 PFU (9.8 days), indicating a delayed disease progression. Despite showing clinical signs of disease and evidence of viral replication as described below, all NHPs challenged i.v. with 5×10^5 or 5×10^4 PFU or i.b. with 5×10^4 PFU MPXV resolved infection. Clinical presentation and progression are summarized in Fig. 1.

The common reports of interstitial pneumonia as a complication of clinical human smallpox prompted our interest in monitoring signs of respiratory disease in all study NHPs inoculated i.v. or i.b. (1, 26). However, due to limitations within our animal biosafety level 3 (ABSL-3), we were unable to directly evaluate NHPs for indications of pneumonia or similar respiratory illness. To address these issues, we measured respiratory rate and oxygen saturation and performed daily observations of the NHPs. The data indicate that little change in the efficiency of the respiratory system was evident in the NHPs inoculated i.v. with 5×10^7 PFU. Oxygen saturation in circulating blood at the peripheral tissues (SpO_2) and respiratory rates remained well within normal limits. NHPs given 5×10^6 PFU i.v. demonstrated elevations in respiratory rates, while SpO_2 remained within normal limits. In contrast to the i.v. inoculated NHPs, the 5×10^6-PFU i.b. inoculated NHPs demonstrated an elevated respiratory rate beginning 5 days postinoculation. The respiratory rate remained elevated in NHPs that succumbed to infection (days 19 and 21 postinoculation) or began to return to near-normal levels by day 16 in the surviving NHP within this group. SpO_2 dropped by day 14 in both moribund 5×10^6-PFU i.b. NHPs and rebounded prior to the NHPs becoming moribund. NHPs in the 5×10^5-PFU i.b. group also developed respiratory symptoms, as evidenced by increased respiratory rates, but again SpO_2 levels remained well within normal limits (Table 2). This suggests that while respiratory effects were more severe in the i.b. inoculated animals, the NHPs remained well oxygenated, which limits the impact that the direct lung damage observed at necropsy (see below) may have had on lethality. Daily observations also indicated respiratory distress in i.b. inoculated NHPs, with coughing and/or dyspnea observed between days 5 and 21. However, it should be noted that coughing or other symptoms were not restricted to the i.b. inoculated NHPs but were more common than for i.v. inoculated NHPs.

Fever, a prominent feature of human MPXV and variola virus infection, was monitored as a parameter to determine disease onset, duration, and severity (Table 3). Eighty-three percent of NHPs inoculated i.v. with 5×10^7 PFU developed fever (defined as a 2°F increase from the NHP's day zero reading) by mean day 3 and lasting until mean day 11 of the study. Surprisingly, the sole survivor from this dosage group did not develop a fever throughout the course of the study, despite becoming viremic and developing skin lesions. Although temperature increases were detected, only one of six NHPs infected with 5×10^6 PFU i.v. and no NHPs at the two lower i.v. doses developed fever as defined here. In contrast, 100% of NHPs infected with 5×10^6 PFU i.b. developed fever with a mean peak (103.9°F) equivalent to that of the 5×10^7-PFU i.v. group. The mean day of fever onset for the NHPs

TABLE 2. Comparison of respiratory parameters in i.v.- and i.b.-inoculated NHPs

Route	Dose (PFU)	Mean peak respiratory rate, breaths per min (range, day 0 mean)	Mean day of peak respiratory rate (range)	Mean value of lowest SpO_2[a] recorded (day 0 mean value, range of change)	Mean day of lowest recorded SpO_2 (range)
i.v.	5×10^7	34.3 (28–44, 26.7)	5.8 (2–10)	94.3[b] (97, 92–98)	6.7[b] (3–14)
	5×10^6	45.3 (32–84, 29.3)	5.5 (2–10)	97.3[b] (96, 94–99)	11.3[b] (9–11)
i.b.	5×10^6	114.7 (100–124, 28)	8.0 (5–14)	94.7[b] (97, 92–99)	12.3[b] (9–14)
	5×10^5	58.4 (36–80, 31.2)	9.4 (8–11)	95.4[c] (94.6, 91–99)	11[c] (5–21)

[a] SpO_2 is the measurement of oxygen saturation in circulating blood at the peripheral tissues.
[b] $n = 3$.
[c] $n = 5$.

TABLE 3. Comparison of fever development in NHPs infected by the intravenous or intrabronchial route

Dose (PFU)	i.v. inoculation				i.b. inoculation			
	No. with fever[a]/no. challenged	Mean day of fever onset[b] (range)	Mean peak temp (°F)	Range of mean peak temp (°F)	No. with fever/no. challenged	Mean day of fever onset (range)	Mean peak temp (°F)	Range of mean peak temp (°F)
5×10^7	5/6	2.6 (2–5)	103.8	102.2–104.1	Not done			
5×10^6	1/6	3.0 (NA)	102.8	102.0–103.6	3/3	6.3 (5–7)	103.9	102.9–104.5
5×10^5	0/3	NA	101.9	101.7–102.3	4/6	7.0 (4–11)	103.5	102.1–104.3
5×10^4	0/3	NA	101.9	101.7–102.3	2/3	6.0[c]	104.2	103.7–104.6

[a] Fever defined as a 2°F increase from the day 0 reading. The mean temperature of all NHPs at day 0 was 101.2°F.
[b] NA, not applicable.
[c] Both NHPs developed fever on day 6.

infected with 5×10^6 PFU i.b. (day 6.3) was delayed more than 2-fold compared to that of NHPs infected with 5×10^7 PFU i.v. (2.6 days). Unlike the NHPs in the 5×10^5- and 5×10^4-PFU i.v. groups, which did not develop fever, 66% of NHPs challenged with either 5×10^5 or 5×10^4 PFU i.b. developed fever.

Lesion development, one of the hallmarks of MPXV and variola virus infection, is used to gauge disease severity in humans using a four-level scale defined by the World Health Organization. The development of skin lesions in relationship to viremia demonstrates that both inoculation routes resulted in a rapid spread of virus to surrounding tissue, resulting in moderate to severe lesional disease (Fig. 2 and Table 4). The mean peak lesion count, day of lesion appearance, and peak day of lesion count of the i.v. and i.b. groups correlated strongly with the dosage level, although the number of lesions that developed varied widely within groups (Table 4). While the mean peak lesion count in NHPs infected with 5×10^6 PFU i.b. was 3-fold less than that observed in NHPs infected with 5×10^7 PFU i.v., the mean day of lesion appearance and mean day of peak lesion count again was delayed compared to that of i.v. inoculation. It should be noted that the 5×10^7-PFU i.v. NHPs that succumbed prior to day 9 developed limited lesional disease, supporting previous work that suggests that a secondary viremia results in skin lesions (5, 26). NHPs that succumbed earlier to infection did not develop as severe a lesional disease as those that survived longer, and this phenomenon accounts for much of the variability observed in the 5×10^7-PFU i.v. group. In the 5×10^5-PFU i.b. group, much variability also was observed in lesion counts, and the NHP that succumbed had the most severe lesional disease. The NHPs receiving 5×10^6 PFU, regardless of route, developed a similar lesional disease that did not partition with outcome.

Ideally, a model of MPXV infection should lead to significant morbidity and mortality to facilitate the study of disease pathogenesis and the testing of countermeasures against severe disease. Therefore, the remainder of the manuscript will focus on the inoculation groups that had at least one moribund NHP: 5×10^6 PFU i.v., 5×10^7 PFU i.v., 5×10^5 PFU i.b., and 5×10^6 PFU i.b.

Viral load in the blood and oral and nasal swabs. Viremia, or viral load in circulating blood, was measured by qPCR as described in Materials and Methods. The mean peak viremia was dose dependent in NHPs infected by the i.v. route but not by the i.b. route (Table 1). The time to the initial detection of viremia did not appear to differ between the i.v. and i.b. groups (Fig. 2), suggesting that virus entry into the bloodstream is rapid by i.b. inoculation as well. However, the viral load when first detected in the blood demonstrated some dose dependence,with the 5×10^7-PFU i.v. NHPs with 5.5 $\log_{10}$ gene copies/ml, 3.8 $\log_{10}$ gene copies/ml detected in the 5×10^6-PFU i.v. NHPs, 4.5 $\log_{10}$ in the 5×10^6-PFU i.b. NHPs, and the 5×10^5-PFU i.b. NHPs having 2.3 $\log_{10}$ gene copies/ml on average. The higher early load of the 5×10^7-PFU i.v. NHPs further supports that i.v. inoculation accelerates disease progression. The mean day of peak viremia for NHPs in the 5×10^6-PFU i.b. group (13.7 days) was delayed compared to that of the 5×10^7-PFU i.v. group (8.2 days) (Table 1), indicating that the route of exposure does impact the severity and progression of disease. Little to no dose dependence was observed between the two doses of i.b. inoculation, but this was due mainly to one NHP that succumbed rather quickly and recorded the highest viremia of any NHP in this study (9.3 $\log_{10}$ gene copies/ml).

Figure 2 compares the development and duration of viremia and lesions in the groups inoculated with 5×10^7 PFU i.v., 5×10^6 PFU i.v., 5×10^6 PFU i.b., and 5×10^5 PFU i.b. While viremia was detected consistently by day 2 or 3 in each group, the development of lesions was dose dependent and followed the onset of viremia by at least 2 days for the 5×10^7-PFU i.v. group, 4 days for the 5×10^6-PFU i.v. and i.b. groups, and 7 days for the 5×10^5-PFU i.b. group. Lesions were largely resolved by day 22 for all surviving NHPs, except for the sole survivor in the 5×10^7-PFU i.v. group. However, all lesions were resolved, and viremia was not detectable by study end on day 36.

Viral shedding at the nasal and oral mucosa is known to be the primary mediator of variola transmission and has been implicated in MPXV transmission (24, 30). Therefore, it was of particular interest to compare viral shedding in NHPs infected by both inoculation routes by the plaque assay of nasal and oral swabs as described in Materials and Methods (Table 5). Although it must be noted that wide variation was observed within groups, mean peak virus titer in nasal swabs was consistent among all of the groups, ranging from 5.1 to 5.6 $\log_{10}$ PFU/ml, indicating systemic virus spread and potential for transmission by both inoculation routes. The onset and peak virus titer of nasal swabs from the 5×10^6-PFU i.b. group, but not the 5×10^5-PFU i.b. group, was delayed by 5 and 3 days, respectively, compared to those of the 5×10^7-PFU i.v. group. In contrast to the nasal swabs, the virus kinetics and peak virus titer in oral swabs demonstrated wider variation between

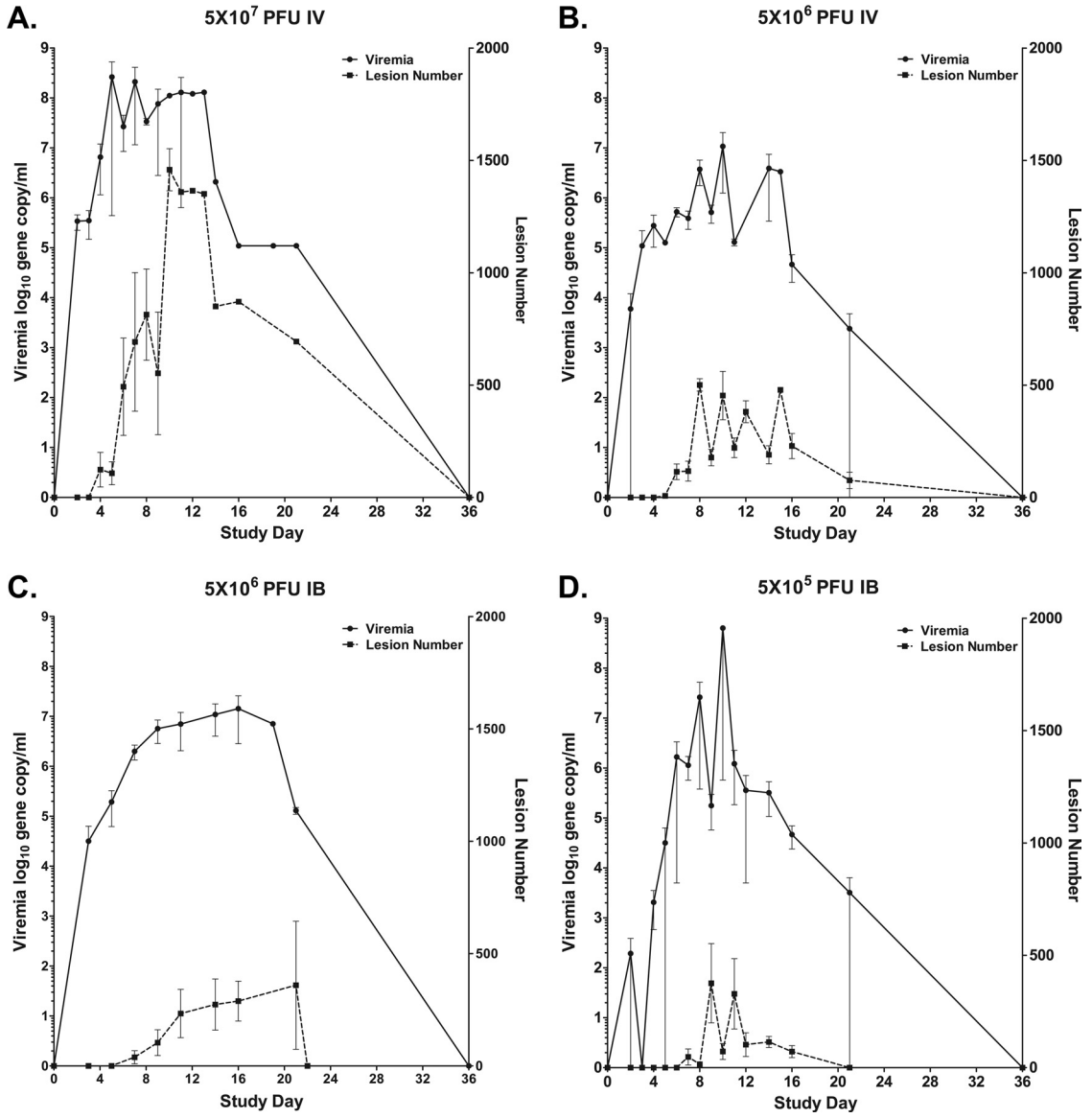

FIG. 2. Mean viremia and lesion counts of infected NHPs. Blood was collected from animals infected by the i.v. or i.b. route at the indicated doses and screened for viral load by qPCR. The number of skin lesions was counted during periodic physical examination.

groups. The 5×10^6- and 5×10^7-PFU i.v. groups had detectable virus by study day 2 to 4, with a peak level of 4.4 and 5.0 $\log_{10}$ PFU/ml, respectively, occurring on day 9. In NHPs infected by the i.b. route, the peak level of MPXV in oral swabs was slightly delayed in the 5×10^6-PFU i.b. group compared to that of the 5×10^5-PFU i.b. group (day 12.0 versus 9.5), and peak virus titers were lower (4.2 and 2.4 $\log_{10}$ PFU/ml) for the 5×10^6- and 5×10^5-PFU i.b. groups, respectively. Both nasal

TABLE 4. Comparison of lesion development in NHPs infected by the intravenous or intrabronchial route

Dose (PFU)	i.v. inoculation				i.b. inoculation			
	Mean peak no. of lesions	Range	Mean day of lesion appearance (range)	Mean day of peak lesion no. (range)	Mean peak no. of lesions	Range	Mean day of lesion appearance (range)	Mean day of peak lesion no. (range)
5×10^7	865	60–1,552	4.5 (2–5)	8.5 (5–10)	Not done			
5×10^6	382	134–661	5.3 (4–7)	10.3 (8–11)	288	194–644	7.6 (7–9)	14.6 (14–21)
5×10^5	93	52–119	6.0[a]	12.0[b]	237	13–615	9.1 (6–11)	11.3 (8–14)
5×10^4	13	0–23	9.0 (8–10)	14.0 (12–16)	170	34–443	8.0 (6–10)	14.6 (12–16)

[a] All 5×10^5-PFU i.v. NHPs developed lesions on day 6.
[b] All 5×10^5-PFU i.v. NHps had peak lesion number on day 12.

TABLE 5. Comparison of viral load in nasal and oral swabs

Route	Dose	Oral swabs			Nasal swabs		
		Mean peak virus titer[a] (log_{10} PFU/ml)	Mean day of initial detection (range)	Mean day of peak virus titer (range)	Mean peak virus titer (log_{10} PFU/ml)	Mean day of initial detection (range)	Mean day of peak virus titer (range)
i.v.	5×10^7	4.4 (3.3–5.1)	4.5 (2–7)	9.0 (5–12)	5.6 (4.6–6.0)	4.8 (4–6)	8.8 (5–12)
	5×10^6	5.0 (3.0–5.7)	5.2 (4–7)	9.6 (6–14)	5.1 (3.3–5.9)	8.2 (7–10)	12.5 (8–21)
i.b.	5×10^6	4.2 (3.0–4.4)	7.0 (5–9)	12.0 (11–14)	5.4 (5.3–5.5)	9.7 (7–9)	11.3 (9–14)
	5×10^5	2.4 (2.0–2.8)	7.2 (5–9)	9.5 (8–12)	5.3 (3.3–5.9)	6.8 (5–10)	7.5 (5–12)

[a] Viral load determined by the plaque assay of nasal and oral swabs on BSC-1 cells.

and oral swabs were largely clear of detectable virus by day 21 postinfection in surviving NHPs.

Viral load in tissues. The distribution of viral load in selected tissues was assessed for NHPs that met the euthanasia criteria of the 5×10^6-PFU i.v. ($n = 1$), 5×10^7-PFU i.v. ($n = 3$ for the comparison, as tissue could not be harvested from two NHPs), and 5×10^6-PFU i.b. ($n = 2$) groups. At the time of necropsy, tissue samples were excised, homogenized, and analyzed by plaque assay on BSC-1 cells (Fig. 3). In general, the distribution and level of virus replication in the analyzed tissues was comparable between the NHPs in the 5×10^7-PFU i.v. and 5×10^6-PFU i.b. groups, although virus titers typically were higher in the i.v. group in lymphoid and reticuloendothelial tissues. In contrast, the sole moribund NHP from the 5×10^6-PFU i.v. group had detectable virus in 5 of the 19 tissues presented, including lung, submandibular lymph node, sternal bone marrow, and tongue, suggesting that the systemic virus spread seen in the 5×10^7-PFU i.v. group was dose dependent.

While i.b. inoculation directly seeds the lungs with virus, it was interesting that lung tissue from the 5×10^7-PFU i.v. group demonstrated similar levels and spread of infectious virus in the various lung tissues that were analyzed (Fig. 3A).

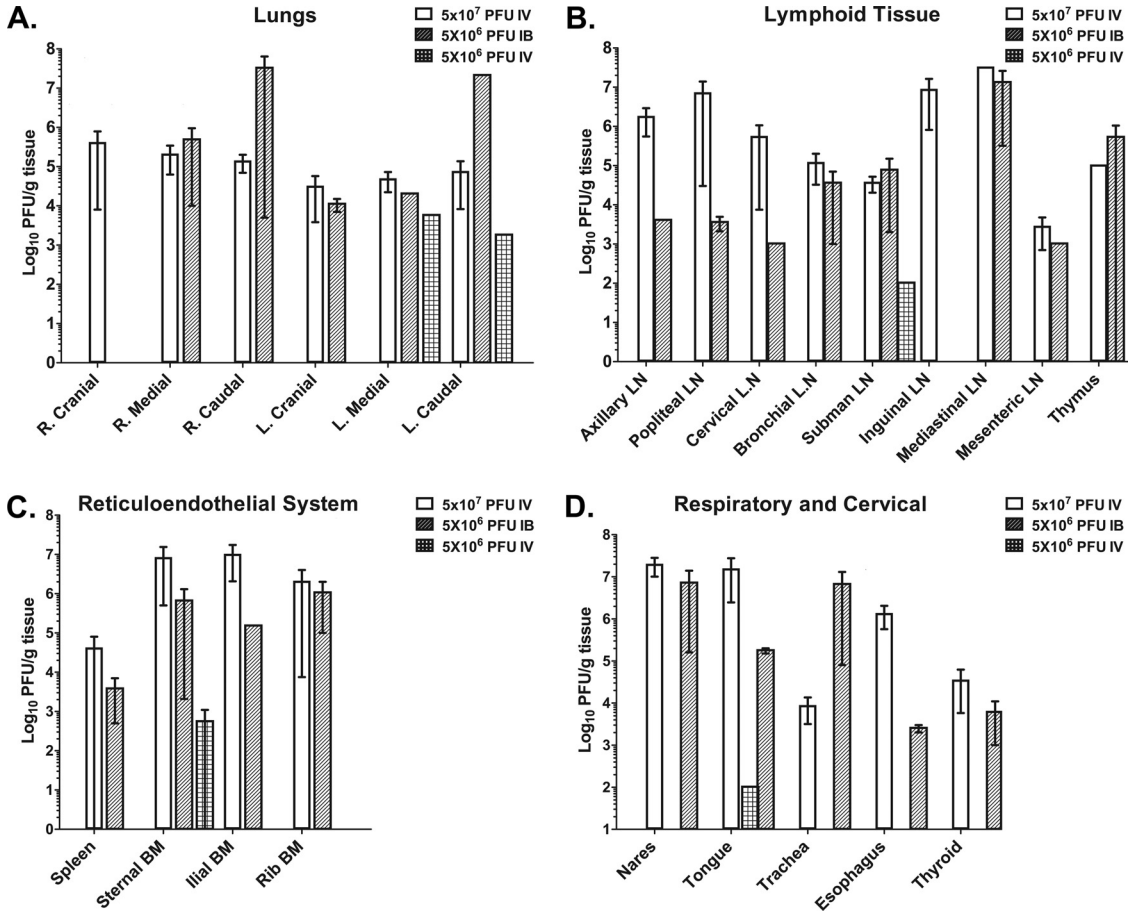

FIG. 3. Mean viral load in tissues. Tissue samples were collected during the necropsy of animals that succumbed to disease and homogenized in PBS to make either 10 or 20% (wt/vol) preparations. The viral load in the tissue homogenates then was measured by plaque assay on BSC-1 cells.

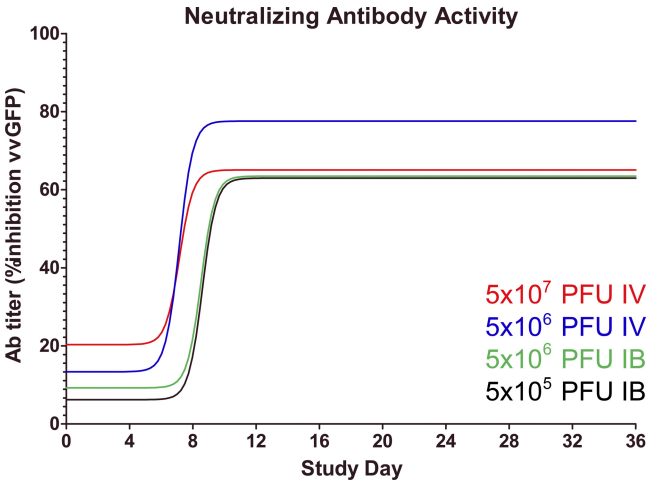

FIG. 4. Neutralizing antibody activity. Antibody production was assayed using a flow cytometric assay of vaccinia GFP fluorescence in infected cells. Data shown are the nonlinear regression of the average titers for animals on a given day.

The 5×10^7-PFU i.v. group had mean virus titers of approximately 5.0 $\log_{10}$ PFU/g in all six lung lobes, while i.b. inoculated NHPs had detectable virus in five of six lung lobes with considerably higher virus levels in the left and right caudal lobes. Notable differences in virus level were observed in the axillary, popliteal, and cervical lymph nodes, where the mean virus titers were greater than 100-fold higher in the 5×10^7-PFU i.v. group compared to those of the 5×10^6-PFU i.b. group (Fig. 3B).

Tissues of interest with the less frequent detection of high levels of virus replication included liver, testes, ovaries, uterus, kidney, and spinal cord.

Development of neutralizing antibody activity. To measure the development of acquired immunity to MPXV, we evaluated the presence of neutralizing antibody activity by a flow cytometry assay using VACV-GFP (Fig. 4). Neutralizing antibody could be detected by approximately day 5 or 6 in the 5×10^7- or 5×10^6-PFU i.v. groups, respectively, and was delayed by approximately 2 days in the i.b. groups. Peak neutralizing antibody activity was similar among the groups in this assay and persisted in nonsurvivors until the study's end. There was no difference detected in the onset or peak antibody activity between survivors or nonsurvivors across the routes or doses tested.

Effect of MPXV infection on cytokine and chemokine levels. Analysis of cytokine and chemokine levels at periodic blood draws during the study indicated that the overall response to infection was proinflammatory. As shown in Table 6, 10 cytokines and chemokines (interleukin-1ra [IL-1ra], IL-2, IL-6, IL-8, gamma interferon [IFN-γ], monocyte chemoattractant protein 1 [MCP-1], RANTES, granulocyte colony-stimulating factor [G-CSF], granulocyte-macrophage CSF [GM-CSF], and sCD40L) demonstrated a measurable increase through the course of the study. The levels of cytokines and chemokines detected in NHPs within groups were highly variable. Cytokines and chemokines that did not increase in concentration during the study included IL-4, IL-5, IL-15, IL-10, IL-12, IL-13, IL-17, IL-18, tumor necrosis factor alpha (TNF-α), MIP-1α, MIP-1β, transforming growth factor alpha (TGF-α), and vascular endothelial growth factor.

The peak fold changes of cytokine/chemokine levels within the i.v. and i.b. groups were largely similar. However, IL-1ra was the only cytokine tested that appeared to have a dramatic difference in peak levels between the i.v. and i.b. groups. The peak fold changes of cytokine/chemokine levels within the two dosage groups of the i.v. and i.b. groups also were similar, with the exception of IL-6, which was dramatically higher in the 5×10^7-PFU i.v. and 5×10^6-PFU i.b. groups. The analysis of the kinetics of cytokine and chemokine responses revealed differences between the 5×10^7-PFU i.v. and 5×10^6-PFU i.b. groups. The mean day of peak cytokine concentrations was delayed approximately 6 days on average for the 5×10^6-PFU i.b. group compared to that of the 5×10^7-PFU i.v. group.

Analysis of PBMCs indicates a shift to proinflammatory cells. The effect of MPXV infection on the PBMC population was assayed by flow cytometry. $CD14^+$ monocytes demonstrated mean 6.1-fold and 7.29-fold increases by days 4.3 and 5 and then returned to baseline levels for the remainder of the study of both the 5×10^6- and 5×10^7-PFU i.v. groups, respectively (Table 7). The 5×10^5- and 5×10^6-PFU i.b. groups had a mean 6.73-fold and 13.33-fold increase in monocytes on days 7.7 and 4.3, respectively. The $CD14^+$ shift persisted longer in the i.b. groups than for the i.v. groups. Shifts in T-cell populations were not as dramatic (Table 7) and were measured as a percentage of $CD3^+$ $CD45^+$ cells. $CD8^+$ T cells did not appreciably shift in moribund NHPs from the 5×10^7-PFU i.v. group. However, the surviving NHP showed a gradual rise beginning at day 9 and persisting until study end. The 5×10^6-PFU i.b. group had the greatest shift in $CD8^+$ T cells, with a peak average of 1.9-fold increase at day 12.67. Differences in the $CD8^+$ T-cell populations in NHPs in the two lower dosage groups were relatively unchanged. $CD4^+$ T-cell levels decreased in each group, with the largest decrease observed in the 5×10^6-PFU i.b. group with an average 0.66-fold change at day 13.3 average. For the 5×10^7-PFU i.v., 5×10^6-PFU i.v., and 5×10^5 PFU i.b. groups, the changes were largely short lived on a subject-by-subject basis.

Select necropsy and histopathology findings. Histopathological examination was performed on the same tissues as those that were selected for plaque assay comparisons. Lung and lymph nodes were the primary focus due to differences in the inoculation route, degrees of lymphadenopathy, and high viral titers observed between the groups.

By gross examination, the lungs of the 5×10^7-PFU i.v. group typically appeared relatively normal, with few subpleural lesions (Fig. 5A). The histological examination of these lungs showed moderate to marked pneumonia consisting primarily of interstitial monocytic and granulocytic inflammation and edema with areas of pulmonary necrosis. Lungs from other NHPs in the 5×10^7-PFU i.v. group were similar to that of the NHP shown in Fig. 5A, with the major consistent finding of interstitial pneumonia of monocytic and granulocytic infiltration coupled with edema and areas of pulmonary necrosis. The NHP shown was selected for euthanasia based on the combination of moderate anorexia, recumbancy, and nonresponsiveness and demonstrated little to no respiratory distress. The gross examination of the lungs from the moribund NHPs in the 5×10^6-PFU i.b. group varied. One moribund NHP demon-

TABLE 6. Cytokine levels indicate a predominantly proinflammatory response

Cytokine/chemokine	Route	Dose (PFU)	Mean day of cytokine peak	Range (days)	Mean peak fold change from day 0	Range (fold change)
IL-1-ra	i.v.	5×10^7	7.0	2–13	4,854	31–25,300
		5×10^6	8.2	2–15	1,855	14–5,553
	i.b.	5×10^6	14.0	7–19	69	3–160
		5×10^5	8.3	4–14	80	2–365
IL-2	i.v.	5×10^7	8.6	6–13	30	10–63
		5×10^6	8.5	3–12	9	2–14
	i.b.	5×10^6	14.0	7–19	18	3–49
		5×10^5	8.2	7–10	20	4–73
IL-6	i.v.	5×10^7	9.6	2–16	1,988	101–9,615
		5×10^6	5.2	3–6	42	11–107
	i.b.	5×10^6	15.7	7–21	3,207	328–9,495
		5×10^5	8.2	7–10	486	82–2,307
IL-8	i.v.	5×10^7	9.2	4–13	73	9–2,798
		5×10^6	10.0	0–16	6	0–10
	i.b.	5×10^6	12.3	9–19	249	2–721
		5×10^5	13.0	8–21	149	2–748
IFN-γ	i.v.	5×10^7	6.7	3–13	400	1–1,167
		5×10^6	3.5	2–5	549	26–1,019
	i.b.	5×10^6	15.6	7–21	442	78–1,042
		5×10^5	7.8	5–10	8,028	44–44,088
MCP-1	i.v.	5×10^7	8.0	5–11	29	7–55
		5×10^6	10.5	8–12	12	4–48
	i.b.	5×10^6	14.0	7–19	30	3–46
		5×10^5	8.7	4–14	441	4–2,307
RANTES	i.v.	5×10^7	5.8	4–10	16	2–49
		5×10^6	7.5	0–16	11	1–25
	i.b.	5×10^6	10.7	9–14	90	2–212
		5×10^5	12.8	8–16	254	5–1,390
GM-CSF	i.v.	5×10^7	10.5	7–35	60	1–297
		5×10^6	8.7	2–16	18	4–45
	i.b.	5×10^6	16.3	9–21	56	10–93
		5×10^5	10.8	8–14	36	2–120
G-CSF	i.v.	5×10^7	9.2	7–13	515	11–2,083
		5×10^6	11.2	8–16	14	2–27
	i.b.	5×10^6	14.7	9–16	724	3–2,161
		5×10^5	11.2	8–16	266	6–1,486
sCD40L	i.v.	5×10^7	7.7	5–13	43	1–98
		5×10^6	9.3	5–16	29	0–104
	i.b.	5×10^6	6.7	0–11	9	1–23
		5×10^5	8.8	8–11	29	15–62

strated severe suppurative pneumonia resulting in pulmonary consolidation, abscess formation, pleural adhesions (not shown), and bacteremia, and it succumbed on day 21. The other moribund NHP demonstrated severe pneumonia with consolidation, pleural adhesion, and no bacteremia, and it succumbed on day 19 (Fig. 5B). Both moribund NHPs developed mild to moderate respiratory disease, as evidenced by occasional coughing and mild to moderate dyspnea during obser-

TABLE 7. Effect of MPXV infection on PBMC populations

Route	Dose	Day of avg peak change of $CD14^+$ cells (range)	Fold change of $CD14^+$ cells from day 0 to peak (range)	Day of avg peak change of $CD4^+$ cells (range)	Fold change of $CD4^+$ cells from day 0 to peak (range)	Day of avg peak change of $CD8^+$ cells (range)	Fold change of $CD8^+$ cells from day 0 to peak (range)
i.v.	5×10^7	5.00 (3–9)	7.29 (0.97–16.3)	16.00 (5–36)	0.72 (0.58–0.85)	16.00 (5–36)	1.54 (1.3–1.8)
	5×10^6	4.33 (3–7)	6.10 (2.5–11.5)	8.67 (5–16)	0.84 (0.64–1.21)	15.00 (3–21)	1.04 (0.78–1.56)
i.b.	5×10^6	4.33 (3–7)	13.33 (12–15)	13.33 (3–21)	0.66 (0.55–0.78)	12.67 (3–19)	1.90 (1.7–2.3)
	5×10^5	7.73 (7–9)	6.73 (3.5–11.7)	7.33 (3–16)	0.78 (0.71–0.85)	5.67 (3–11)	1.30 (1.2–1.4)

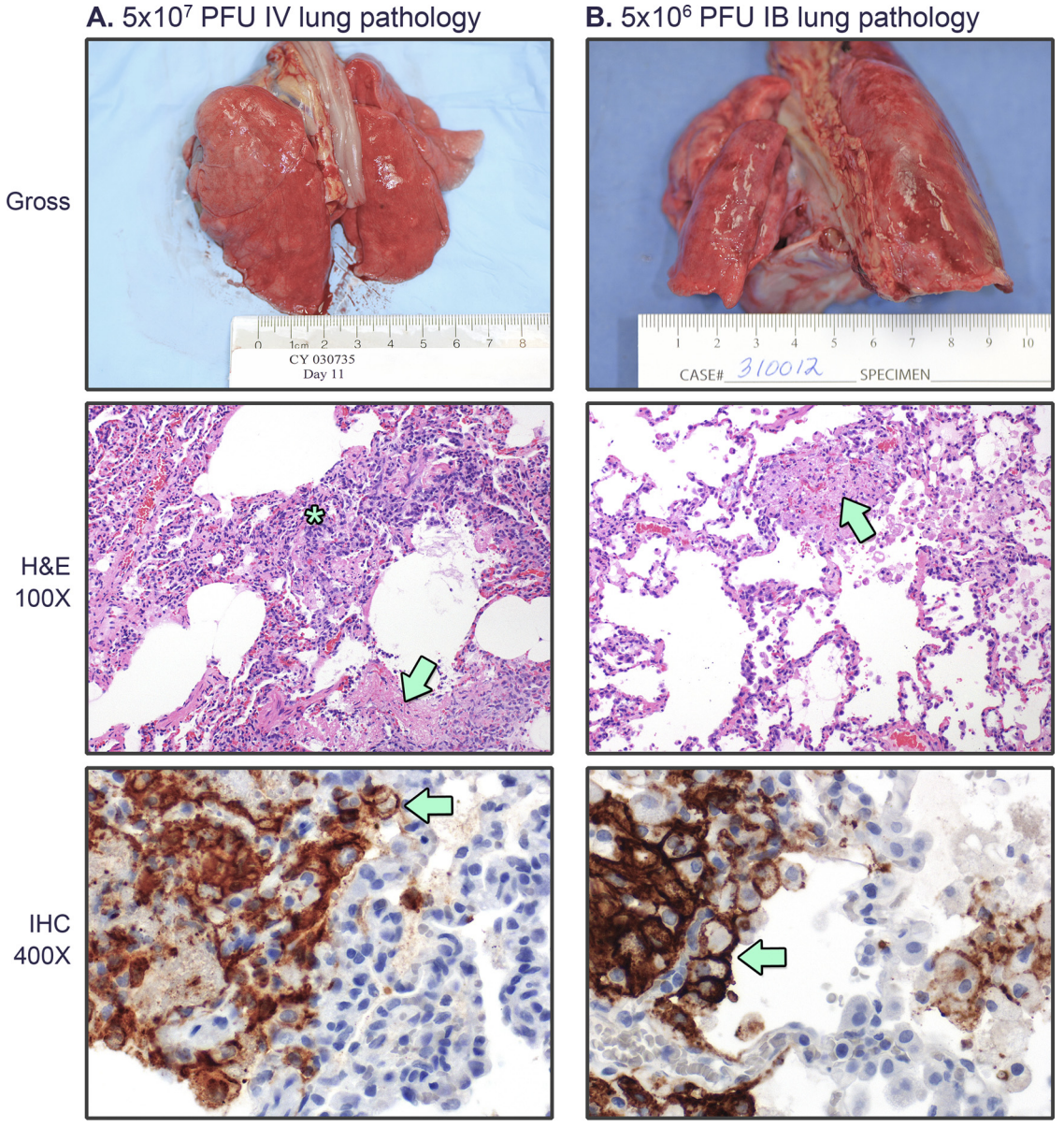

FIG. 5. Lung histopathology. (A) Gross pathology and histopathological examination of lung from an NHP in the 5×10^7-PFU i.v. group harvested at necropsy 11 days postinoculation. H and E, pneumonia consisting of interstitial monocytic and granulocytic inflammation (asterix) and edema with areas of pulmonary necrosis (arrow head); IHC, lung exhibits poxviral antigen immunoreactivity centered around areas of necrosis. (B) NHP from the 5×10^6-PFU i.b. group harvested at necropsy 19 days postinoculation. H and E, pneumonia with areas of necrosis (arrow head) and less inflammation than the i.v. group lungs; IHC, strong poxviral antigen immunoreactivity primarily within the cytoplasm of histiocytes (arrow).

vation or physicals that first was noted 5 days postinoculation and peaked on day 14. The surviving NHP from the 5×10^6 PFU i.b. group also had similar, although less severe, symptoms. Histopathologic analysis demonstrated viral pneumonia with interstitial inflammation, pulmonary consolidation, fibrosis, fibrin deposition, edema, and pleuritis. In both the 5×10^7-PFU i.v. group and the 5×10^6-PFU i.b. group there were instances of significant concomitant bacteremia.

Lymph nodes from NHPs in the 5×10^7-PFU i.v. and 5×10^6-PFU i.b. groups were evaluated grossly and histologically. The lymph nodes shown in Fig. 6 were taken from the same NHPs as those shown in Fig. 5. Specifically, axillary lymph nodes from the 5×10^7-PFU i.v. group often demonstrated gross enlargement (lymphadenopathy) and one or more of the following, histologically: lymphoid necrosis, lymphoid depletion, lymphadenitis, diffuse sinus edema, sinus histiocytosis, neutrophilia, and occasional intracytoplasmic inclusion bodies within histiocytes (Fig. 6A). Axillary lymph nodes from the 5×10^6-PFU i.b. group also were characterized by diffuse lymphadenopathy, and histologically there were active germinal centers and histiocytic phagocytosis of cellular debris within germinal centers and sinuses that also often were edematous.

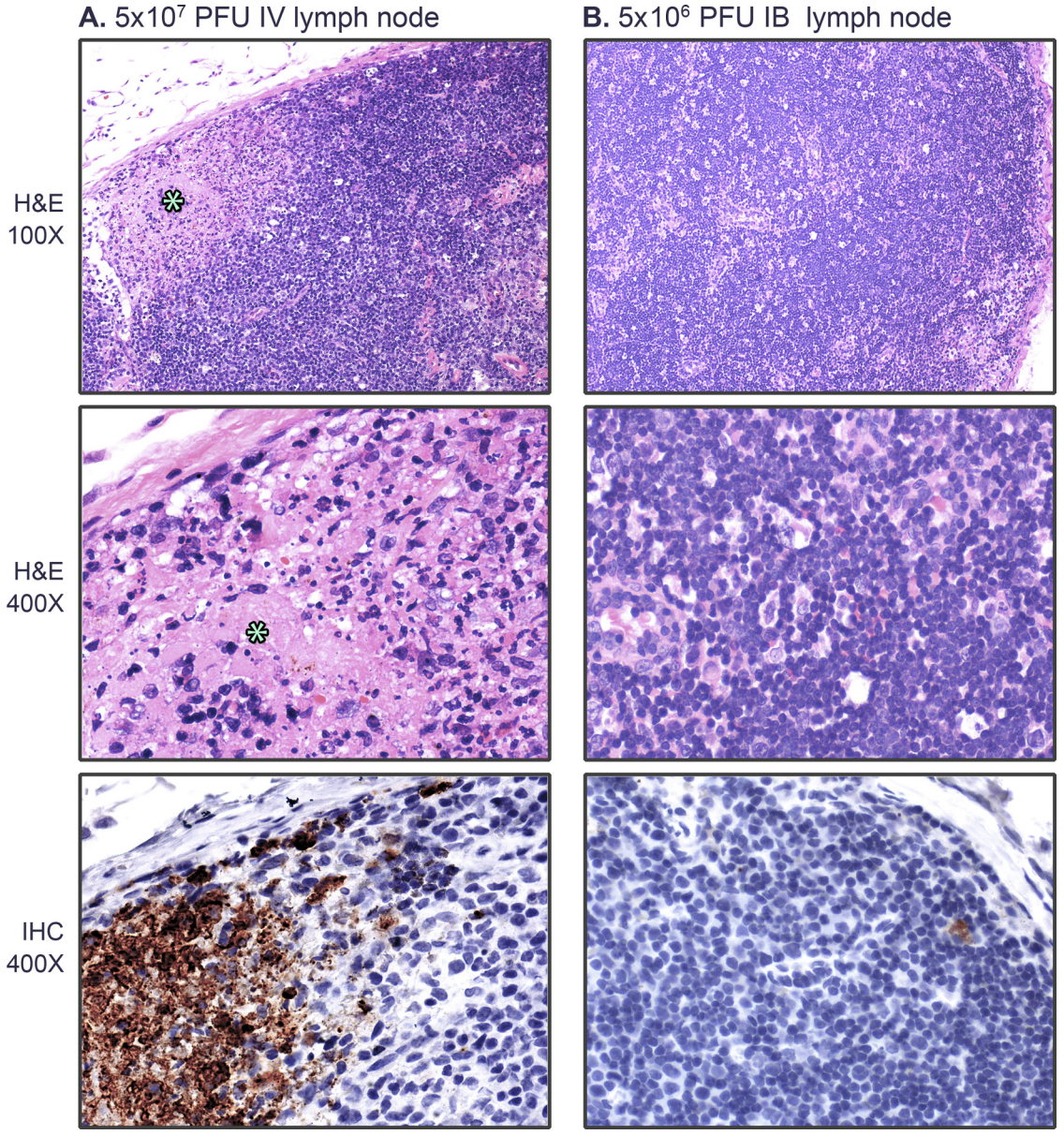

FIG. 6. Lymph node histopathology. Axillary lymph node from (A) an NHP from the 5×10^7-PFU i.v. group collected at necropsy 11 days postinoculation and (B) an NHP from the 5×10^6-PFU i.b. group collected at necropsy 19 days postinoculation. (A) Diffuse enlargement (lymphadenopathy) with multifocal areas of necrosis (asterisk) and histiocytic phagocytosis of cellular debris. IHC indicates that the axillary lymph node exhibits poxviral antigen immunoreactivity within areas of necrosis. (B) Diffuse lymphadenopathy with histiocytic phagocytosis of cellular debris. IHC indicates that the axillary lymph node exhibits rare poxviral antigen immunoreactivity within the cytoplasm of histiocytes within the cortex.

There also was occasional lymphocytolysis (Fig. 6B), and in NHPs that had a concomitant bacterial infection there often was lymphoid necrosis with marked lymphoid depletion and bacterial lymphadenitis (not shown). Other significant gross and histopathologic lesions were noted in all challenge groups and will be reported separately.

DISCUSSION

Our goal was to expand the understanding of monkeypox pathogenesis in the commonly utilized i.v. model and evaluate the i.b. inoculation route as a new model of infection. i.b. inoculation was chosen because it (i) has been reported to be effective for other pathogens (4, 23, 27), (ii) may prove to be more reliable and accessible than aerosol inoculation, and (iii) more closely resembles the natural route of infection (respiratory exposure) than i.v. inoculation (15). It is believed that the i.v. inoculation of NHPs with MPXV bypasses key events early in infection during the incubation phase that may determine the severity of clinical disease. In fact, the i.v. inoculation of NHPs with 5×10^7 PFU results in fever and lesion development by mean day 3 and 5, respectively. This is in contrast to

human cases of MPXV and variola infection, where fever, malaise, prostration, and subsequent lesion development typically follow an approximately 12-day incubation phase after exposure (13, 31). It was hypothesized that peripheral exposure, such as by i.b. inoculation, serves to extend the incubation phase and delay the progression of disease, since the bloodstream was not directly seeded with a large dose of virus. The direct seeding of the bloodstream by i.v. inoculation results in the greater accessibility of the virus to target organs, resulting in a rapid disease course. In the current study, the time to the onset of fever was more than doubled when the two high-dose groups were compared, the 5×10^7-PFU i.v. group (2.6 days) and 5×10^6-PFU i.b. group (6.3 days). In addition, the time to lesion appearance was delayed by 3 days, from 4.5 days for the 5×10^7-PFU i.v. group to 7.6 days for the 5×10^6-PFU i.b. group. Thus, the incubation phase did appear to be extended for i.b. inoculation, although it did not reach the length of time reported to be standard for human infection. Somewhat surprisingly, the time to the detection of viremia was equivalent between the two routes. These results nevertheless are an improvement in the model and were coupled with delays in time to (i) peak viremia levels, (ii) peak lesion development, (iii) peak cytokine levels, and (iv) reaching endpoint criteria. Such findings suggest that i.b. inoculation allows the study of disease events that are eclipsed by i.v. inoculation and more accurately reflects human disease.

The levels of virus replication in blood and in tissues were largely similar between the routes evaluated here and were comparable to those previously reported by Huggins et al. and Stittelaar et al. (17, 40). Mean peak viremia was approximately 10-fold lower in the 5×10^6-PFU i.b. and 5×10^6-PFU i.v. groups compared to that of the 5×10^7-PFU i.v. group. Unexpectedly, the 5×10^5 PFU i.b. group had levels of viremia similar to those of the 5×10^7-PFU i.v. group, but this was due mainly to the highest level of viremia (9.3 $\log_{10}$ gene copies/ml) recorded in one moribund NHP from the 5×10^5-PFU i.b. group. Virus dissemination in tissues was influenced by route and dose, with the 5×10^7-PFU i.v. and 5×10^6-PFU i.b. groups demonstrating similar distribution and viral load. Lower doses with either route led to differences in pathogenesis. The involvement of the individual tissue types in overall pathogenesis is difficult to fully understand. Histopathological analysis also supports tissue damage by viral infection in the tissues with high viral load, including lung and lymph nodes. Clearly, the loss of reticuloendoethelial tissues and lymphoid organs either by direct cytocidal effects or secondary effects of infection would contribute to pathogenesis by impairing the ability of the host to combat infection. Virus infection of the lung would provide a means of transmission for the virus, and the resulting pathology also would affect overall health, although O_2 saturation measurements did not directly support this notion. The severe inflammation of the lung was observed in NHPs inoculated by both routes at the two highest doses, suggesting that the lung is a major target organ of MPXV.

The data from both inoculation routes supports the probability of MPXV transmission via an aerosol route, which has been implicated in human-to-human spread (1, 12, 18). The plaque assay of respiratory tract tissues revealed moderate to high viral load at high doses independent of route. We also observed that high levels of infectious virus could be detected in nasal and oral swabs, which is consistent with previously reported data (19, 40). NHPs inoculated with the lower doses by either route also demonstrated moderate to high virus titers in nasal and oral swabs, suggesting that mildly ill NHPs are shedding virus and could support transmission between NHPs or other susceptible animals. Also of note is that NHPs were shedding virus in nasal and oral swabs concomitantly with the onset of fever but prior to the presence of lesions. These observations also may hold true for humans, suggesting that infected people could shed MPXV virus in quantities sufficient to infect another person prior to showing clinical signs.

Overall, we observed a strong proinflammatory response as evidenced by the cytokine data presented, changes in PBMC population, and the development of neutralizing antibodies. The infection with 5×10^6 PFU i.v. and 5×10^5 PFU i.b. was well controlled by the NHPs and may provide further insight into identifying responses that improve survival. Neutralizing antibody activity was observed in all groups, and peak neutralizing antibody activity overlapped the peak viremia for each group for several days prior to the decline in viremia. The analysis of the PBMC populations revealed shifts that also support a proinflammatory response. $CD14^+$ monocytes increased the most, suggesting that the cytokine milieu promoted their development and possible recruitment from regional lymph nodes and tissues to sites of infection. The recruitment of monocytes to inflammation could result in two outcomes: (i) aiding in the clearance of damaged tissue and ultimately virus clearance by acting as an antigen-presenting cell, and (ii) further spreading virus throughout the body as monocytes are thought to be productively infected by orthopoxviruses (14, 33). For the 5×10^7-PFU i.v. NHPs, the proportion of T cells shifted slightly to $CD8^+$ near the endpoint for each of the moribund animals, but it peaked at day 36 for the surviving animal; as this was at the study endpoint, it is difficult to determine the role of $CD8^+$ T cells in the clearance of MPXV. With the other groups a clear trend is less defined, as peaks occurred over a vast range of days and did not necessarily coincide with disease severity. A similar trend was observed for $CD4^+$ cells, but $CD4^+$ cells demonstrated slight decreases. Further studies will be needed to determine the role of T cells in MPXV pathogenesis.

In contrast to previous reports, our data do not support an immunopathology or rampant immune dysregulation similar to what has been suggested for variola virus infection of cynomolgus macaques (21). Instead, we observed a strong proinflammatory response in all groups. NHPs in the 5×10^7-PFU i.v. and 5×10^6-PFU i.b. inoculation groups demonstrated the strongest changes with some differences, such as a stronger response for IL-6, IL-8, and G-CSF in the i.b. NHPs. The proinflammatory response paralleled the onset of viremia for each of the groups. However, the analysis of individual NHPs within each of the groups revealed a wide variation in response among the NHPs for each cytokine. Further definition of trends in the cytokine response may require expanded experimental groups to offset the wide variability in response.

The histopathological analysis of multiple tissues confirmed the spread of virus throughout the infected NHPs and, in particular, damage to epithelial regions. As observed in human disease, generalized lymphadenopathy was a fairly consistent finding between the two routes of inoculation; however, there

were variations in the severity of lymph node pathology both between and within groups. Lymph nodes taken from i.v. inoculated NHPs that succumbed indicated lymphadenopathy due to lymphoid necrosis, lymphoid depletion, and the congestion of the lymphatics. Lymph nodes from i.b. inoculated NHPs and i.v. inoculated NHPs that survived demonstrated lymphadenopathy due to lymphoid hyperplasia and the development of germinal centers. The severity and types of pneumonia also varied between the inoculation routes. Histopathologic findings of the 5×10^7-PFU i.v. group lungs indicated interstitial pneumonia, which has been noted previously (34); within the 5×10^6-PFU i.b. group lungs, while there was some interstitial pneumonia present, there was also a necrotizing bronchopneumonia and, in one case, a suppurative pneumonia. The gross and histopathologic observations support and are consistent with the coughing and labored breathing observed in the i.b. group.

Furthermore, bronchopneumonia was reported as the most common disease complication of human smallpox, but it is unclear if bronchopneumonia was directly caused by VARV or a secondary bacterial infection (5). Support for bronchopneumonia as a direct consequence of infection rather than a secondary bacterial infection comes from data that indicates that the mortality rate did not change after the advent of antibiotics (5, 26). Our results indicate that bronchopneumonia is a direct result of MPXV infection, as six out of six NHPs in the 5×10^7-PFU i.v. group developed interstitial pneumonia. However, of these six, two were bacteremic, and the bacteremia was not specific to the lungs. Of the two animals within the 5×10^6-PFU i.b. group that succumbed, 1 NHP was bacteremic and the other was not, but both had indications of severe pneumonia. We cannot conclusively rule out that MPXV infection did not predispose the severely affected animals to secondary bacterial infections that resulted in a suppurative bronchopneumonia, lymphoid necrosis, and depletion. It is possible that the ulcerated poxviral skin lesions, or administering the agent via the i.b. route, caused a severe localized inflammatory response with subsequent tissue disruption resulting in opportunistic bacteria gaining vascular access, eventually causing sepsis in susceptible NHPs. Secondary bacterial infections have been reported in other NHP MPXV studies (34, 43) and, importantly, in clinical reports of smallpox (3, 26). We chose to report and include bacteremic animals in our study, as secondary bacterial infections and other concomitant infections have been reported to contribute to MPXV (2) and variola disease in human cases that result in death (3, 26). Considering the importance of the skin and epithelial barriers in protection against bacterial infections, it is not surprising that a disease that causes severe damage to the skin and other epithelia would result in secondary bacterial infection or sepsis.

Secondary bacterial infection may complicate immunological and pathological findings and make viral pathogenesis difficult to distinguish from overall disease pathogenesis. However, it needs to be considered that sepsis and other secondary infections may be a common feature of MPXV infection. Nevertheless, the high levels of virus replication and detection of viral antigen in the affected tissues indicate that MPXV replication was critical in the development of disease. Studies involving MPXV infection with and without intentional bacterial infection could help determine the role of bacterial infection in overall disease pathogenesis.

It has been reported that the MPXV infection of humans also is influenced by the route of inoculation. Reynolds et al. demonstrated that during the 2003 U.S. outbreak of the west African clade MPXV, the route of inoculation corresponded to the severity and spread of disease. Humans who had a complex exposure (evidence of scratch or bite) had more severe disease with an earlier onset by 5 days compared to a noninvasive exposure route (30). Recent investigations using aerosol, intratracheal (i.t.), and intranasal (i.n.) MPXV administration provide further support that the route of inoculation plays a role in disease progression (34, 38, 39, 40, 43). i.n. inoculation resulted in limited systemic classical pox disease, with no mortality (34). When the results of the 5×10^6-PFU i.b. group reported herein are compared to those from NHPs administered 2.5×10^6 PFU i.t. (39), the NHPs from the i.t. route had a higher mean mortality rate (100%) but a shorter time to death (16.3 days i.t. [39] versus 20 days i.b.). Viremia was similar, with 6.5 $\log_{10}$ gene copies/ml for the i.t. route and 6.3 $\log_{10}$ gene copies/ml for the i.b. route. Histopathological analysis indicates similar lung pathology, with fibronecrotic bronchopneumonia reported in both models. When the aerosol challenge route is compared to i.b. and i.t. routes, NHPs met euthanasia criteria at 10 days and have similar virus distribution, viremia, and bronchopneumonia with pleuritis. Thus, it is unclear whether any of the respiratory exposure models can be considered superior at this time. The further improvement of the i.b. methodology may provide a repeatable, easily accessible respiratory model for MPXV infection. Future studies would involve the modification of the inoculum and flush volumes and the further characterization of the pneumonia observed by both routes using molecular imaging techniques, such as positron emission tomography/computed tomography. Once these issues are addressed, larger study group sizes would be available to provide statistical significance to the observations.

Overall, we were able to demonstrate that the i.b. inoculation route resulted in a classical pox-like disease with similarities to the commonly used i.v. model in terms of clinical, virological, and immunological parameters. Several key events were delayed in the highest doses tested of the i.b. model compared to those of the i.v. model, including the onset of (i) fever and lesion appearance, (ii) peak viremia, (iii) viral shedding in nasal and oral swabs, (iv) peak cytokine levels, and (v) endpoint criteria. Our data suggest that the 5×10^6-PFU i.b. model provides insight into pathogenesis that may be lost by the rapid severity of the 5×10^7-PFU i.v. model, and that the i.b. model should be considered for further studies of viral pathogenesis and countermeasures.

ACKNOWLEDGMENTS

This study was supported, in part, by the NIAID Division of Intramural Research.

We are grateful to Sharon Altman, Abigail Lara, Sarah Rovezzi, Jason Clardy, and Daena Carrera for technical assistance. We are grateful to Laura Bollinger and Fabian De Kok Mercado for assistance in preparation of the manuscript.

REFERENCES

1. **Arita, I., and D. A. Henderson.** 1968. Smallpox and monkeypox in non-human primates. Bull. World Health Organ. **39:**277–283.

2. **Arita, I., et al.** 1985. Human monkeypox: a newly emerged orthopoxvirus zoonosis in the tropical rain forests of Africa. Am. J. Trop. Med. Hyg. **34:**781–789.
3. **Breman, J. G., and D. A. Henderson.** 2002. Diagnosis and management of smallpox. N. Engl. J. Med. **346:**1300–1308.
4. **Brody, S. L., et al.** 1994. Acute responses of non-human primates to airway delivery of an adenovirus vector containing the human cystic fibrosis transmembrane conductance regulator cDNA. Hum. Gene Ther. **5:**821–836.
5. **Chapman, J. L., et al.** 2010. Animal models of orthopoxvirus infection. Vet. Pathol. **47:**852–870.
6. **Chen, N., et al.** 2005. Virulence differences between monkeypox virus isolates from West Africa and the Congo basin. Virology **340:**46–63.
7. **Di Giulio, D. B., and P. B. Eckburg.** 2004. Human monkeypox: an emerging zoonosis. Lancet Infect. Dis. **4:**15–25.
8. **Earl, P. L., et al.** 2004. Immunogenicity of a highly attenuated MVA smallpox vaccine and protection against monkeypox. Nature **428:**182–185.
9. **Earl, P. L., J. L. Americo, and B. Moss.** 2003. Development and use of a vaccinia virus neutralization assay based on flow cytometric detection of green fluorescent protein. J. Virol. **77:**10684–10688.
10. **Edghill-Smith, Y., et al.** 2005. Smallpox vaccine does not protect macaques with AIDS from a lethal monkeypox virus challenge. J. Infect. Dis. **191:**372–381.
11. **Edghill-Smith, Y., et al.** 2005. Smallpox vaccine-induced antibodies are necessary and sufficient for protection against monkeypox virus. Nat. Med. **11:**740–747.
12. **Fennerty, M. B.** 1996. Polio and small pox: diseases of historical interest because of vaccines. Will this also apply to Helicobacter pylori? Am. J. Gastroenterol. **91:**170–171.
13. **Foege, W. H., J. D. Millar, and J. M. Lane.** 1971. Selective epidemiologic control in smallpox eradication. Am. J. Epidemiol. **94:**311–315.
14. **Hammarlund, E., et al.** 2008. Monkeypox virus evades antiviral CD4+ and CD8+ T cell responses by suppressing cognate T cell activation. Proc. Natl. Acad. Sci. U. S. A. **105:**14567–14572.
15. **Henderson, D. A., et al.** 1999. Smallpox as a biological weapon: medical and public health management. Working Group on Civilian Biodefense. JAMA **281:**2127–2137.
16. **Hooper, J. W., et al.** 2004. Smallpox DNA vaccine protects nonhuman primates against lethal monkeypox. J. Virol. **78:**4433–4443.
17. **Huggins, J., et al.** 2009. Nonhuman primates are protected from smallpox virus or monkeypox virus challenges by the antiviral drug ST-246. Antimicrob. Agents Chemother. **53:**2620–2625.
18. **Huhn, G. D., et al.** 2005. Clinical characteristics of human monkeypox, and risk factors for severe disease. Clin. Infect. Dis. **41:**1742–1751.
19. **Hutson, C. L., et al.** 2010. Dosage comparison of Congo Basin and West African strains of monkeypox virus using a prairie dog animal model of systemic orthopoxvirus disease. Virology **402:**72–82.
20. **Jahrling, P. B., E. A. Fritz, and L. E. Hensley.** 2005. Countermeasures to the bioterrorist threat of smallpox. Curr. Mol. Med. **5:**817–826.
21. **Jahrling, P. B., et al.** 2004. Exploring the potential of variola virus infection of cynomolgus macaques as a model for human smallpox. Proc. Natl. Acad. Sci. U. S. A. **101:**15196–15200.
22. **Jezek, Z., et al.** 1987. Human monkeypox: clinical features of 282 patients. J. Infect. Dis. **156:**293–298.
23. **Larsen, M. H., et al.** 2009. Efficacy and safety of live attenuated persistent and rapidly cleared Mycobacterium tuberculosis vaccine candidates in nonhuman primates. Vaccine **27:**4709–4717.
24. **Learned, L. A., et al.** 2005. Extended interhuman transmission of monkeypox in a hospital community in the Republic of the Congo, 2003. Am. J. Trop. Med. Hyg. **73:**428–434.
25. **Likos, A. M., et al.** 2005. A tale of two clades: monkeypox viruses. J. Gen. Virol. **86:**2661–2672.
26. **Martin, D. B.** 2002. The cause of death in smallpox: an examination of the pathology record. Mil. Med. **167:**546–551.
27. **Messaoudi, I., et al.** 2009. Simian varicella virus infection of rhesus macaques recapitulates essential features of varicella zoster virus infection in humans. PLoS Pathog. **5:**e1000657.
28. **Parker, S., et al.** 2007. Human monkeypox: an emerging zoonotic disease. Future Microbiol. **2:**17–34.
29. **Reed, K. D., et al.** 2004. The detection of monkeypox in humans in the Western Hemisphere. N. Engl. J. Med. **350:**342–350.
30. **Reynolds, M. G., et al.** 2006. Clinical manifestations of human monkeypox influenced by route of infection. J. Infect. Dis. **194:**773–780.
31. **Ricketts, T. F.** 1910. The diagnosis of smallpox. Funk and Wagnalls, New York, NY.
32. **Rimoin, A. W., et al.** 2010. Major increase in human monkeypox incidence 30 years after smallpox vaccination campaigns cease in the Democratic Republic of Congo. Proc. Natl. Acad. Sci. U. S. A. **107:**16262–16267.
33. **Rubins, K. H., et al.** 2008. Comparative analysis of viral gene expression programs during poxvirus infection: a transcriptional map of the vaccinia and monkeypox genomes. PLoS One **3:**e2628.
34. **Saijo, M., et al.** 2009. Virulence and pathophysiology of the Congo Basin and West African strains of monkeypox virus in non-human primates. J. Gen. Virol. **90:**2266–2271.
35. **Sbrana, E., et al.** 2007. Comparative pathology of North American and central African strains of monkeypox virus in a ground squirrel model of the disease. Am. J. Trop. Med. Hyg. **76:**155–164.
36. **Sbrana, E., et al.** 2007. Efficacy of the antipoxvirus compound ST-246 for treatment of severe orthopoxvirus infection. Am. J. Trop. Med. Hyg. **76:**768–773.
37. **Sofi Ibrahim, M., et al.** 2003. Real-time PCR assay to detect smallpox virus. J. Clin. Microbiol. **41:**3835–3839.
38. **Stittelaar, K. J., et al.** 2001. Safety of modified vaccinia virus Ankara (MVA) in immune-suppressed macaques. Vaccine **19:**3700–3709.
39. **Stittelaar, K. J., et al.** 2005. Modified vaccinia virus Ankara protects macaques against respiratory challenge with monkeypox virus. J. Virol. **79:**7845–7851.
40. **Stittelaar, K. J., et al.** 2006. Antiviral treatment is more effective than smallpox vaccination upon lethal monkeypox virus infection. Nature **439:**745–748.
41. **Tesh, R. B., et al.** 2004. Experimental infection of ground squirrels (Spermophilus tridecemlineatus) with monkeypox virus. Emerg. Infect. Dis. **10:**1563–1567.
42. **WHO.** 2009. Selected priority diseases under weekly surveillance: cases and deaths in 2009. Afr. Health Monit. **11:**56–57.
43. **Zaucha, G. M., et al.** 2001. The pathology of experimental aerosolized monkeypox virus infection in cynomolgus monkeys (Macaca fascicularis). Lab. Investig. **81:**1581–1600.